https://doi.org/10.5194/egusphere-2025-3473
Preprint. Discussion started: 2 October 2025

Forecasting people exposed to tropical cyclone flooding in Southeast Africa: Lessons learned from recent events.

Jeffrey Neal[1], Anthony Cooper[2], Stephen J. Chuter[1], Leanne Archer[1], Laura Devitt[1], Stephen Grey[3], Laurence Hawker[1], James Savage[2], Elisabeth Stephens[5,6], Calum Baugh[4], Tim Sumner[7], Katherine Marsden[7] and Tamara Janes[7,8]

1. School of Geographical Science, University of Bristol, UK
2. Fathom, Bristol, UK
3. HR Wallingford Ltd, Howbery Park, Wallingford, OX10 8BA, UK
4. Forecast and Services Department, ECMWF, Shinfield Park, Reading, UK, RG2 9AX
5. Department of Meteorology, University of Reading, UK
6. Red Cross Red Crescent Climate Centre, The Hague, Netherlands
7. Foreign and Commonwealth Development Office, London, UK
8. MetOffice, Exeter, UK

Corresponding Author: Jeffrey Neal j.neal@bristol.ac.uk

Abstract

East Africa has recently experienced a series of devastating tropical cyclone landfalls characterised by hundreds of fatalities, millions of displaced people and substantial economic damage. Forecasting the impact of these tropical cyclones can, in theory, better motivate anticipatory action compared to only forecasting the hazard. This paper describes an approach to forecasting the number of people directly exposed to flooding from tropical cyclones and documents experience gained communicating these forecasts to practitioners via emergency bulletins.

Forecasting flood exposure requires a complex cascade of meteorological, hydrological, hydraulic and population models. Interpretation of forecasts was difficult, even for the scientific experts developing the systems, due to uncertainties brought in at each stage of the modelling cascade. Thus, producing interpretable forecast messaging was challenging and often required extensive discussion between forecasters with expertise on different elements of the system. This paper uses practical experience gained from several tropical cyclone events to highlight essential requirements for interpreting and disseminating tropical cyclone flood impact forecasts. We also analyse how forecasts evolved with lead-time and compare them to observed flooding in the case of Tropical Cyclone Freddy. Overall, we aim to synthesise our experience into actionable learning that might inform future use of forecasting in humanitarian response.

Exposure estimates were most sensitive to storm track location, even when exposure was aggregated to districts. Uncertainty from track location remained substantial even in the days before landfall, meaning a recipient of these forecasts needs to understand and interpret the distribution of exposure. For the second landfall of Tropical Cyclone Freddy, nationwide exposure estimates were remarkably similar between remotely sensed flood extents and the best estimate from the forecast system. However, this overall similarity results from the averaging of substantial uncertainty at the district scale.

https://doi.org/10.5194/egusphere-2025-3473
Preprint. Discussion started: 2 October 2025

1 Introduction

Flood disasters are pervasive and entrenched in our society. Tropical cyclones can be especially devastating due to their multi-hazard nature and potential to generate exceptional flood magnitudes. In Africa, a combination of high vulnerability to flooding and lack of pre-emptive action can exacerbate disaster risk. For example, in 2019 Tropical Cyclone Idai caused more than 600 fatalities in Mozambique and left over 1.8 million people in need of humanitarian assistance (UNOCHA, 2019). Prevention of flooding is usually not feasible, however accurate and timely impact-based forecasts of tropical cyclone flooding have been called for to support early warning and action to save lives and livelihoods (Nauman, 2021).

Forecasting tropical cyclone track, rainfall, windspeed and river flows has received significant attention (Lu et al., 2024). Several global centres (e.g. European Centre for Medium Range Weather Forecast, National Centres for Atmospheric Research) issue weather forecasts on which severe weather bulletins can be based and ingested by national agencies with mandated responsibilities for warning the public. For example, in the Southwest Indian Ocean Météo France in La Réunion is designated as the Regional Specialised Meteorological Centre for tropical cyclone forecasting by the World Meteorological Organisation. In terms of people exposed to flooding, severe weather bulletins sometimes forecast the number of people indirectly affected by severe weather or heavy rainfall, often summing the total population living under the tropical cyclone track. However, More nuanced estimates of exposure, such as the number of people directly flooded, are often not provided because the data underlying the forecasts does not support such predictions. When exposure estimates are provided, for example by the World Food Program Advanced Disaster Analysis and Mapping (ADAM) platform (https://gis.wfp.org/adam/), ambiguity over exactly what is included is common. Speight et al. (2024) highlight a need for additional data and expertise to support the interpretation of global flood and exposure models, clear documentation to support decision makers faced with multiple sources of information, and the development of user-relevant metrics to assess forecast skill.

A lack of pre-emptive forecast-based action is often cited as a reason for poor outcomes for those impacted by the flooding. While there are many reasons for this, including insufficient capacity to act, there is currently limited capability to make large-scale (e.g. covering the whole tropical cyclone) yet locally-relevant exposure forecasts of people directly affected by flooding (e.g. those whose houses will flood) in Africa. Unlike most other natural hazards, resolution well below 100m is necessary because flood hazard changes materially over a few decimetres and people will avoid settling in hazardous locations if they can (Smith et al., 2019). Recent advances in global flood hazard mapping can theoretically provide inundation depth estimates with sufficient resolution (~30 m) to estimate community level flood exposure when combined with high-resolution population data (Hawker et al., 2024; Wing et al., 2024). However, errors can be substantial at such fine resolutions and early large-scale flood models (often at 1 km resolution) faced a credibility challenge due to simulating divergent estimates of flood extent (Trigg et al., 2016). Improvements to these models, notably the underlying terrain data (Hawker et al., 2022) mean they might, for the first time, be able to support district level hazard and exposure forecasts. However, these forecasts will be complicated by substantial uncertainties, meaning interpretation and use of these data requires significant care.

This study evaluates tropical cyclone forecasts that underpin a pilot emergency bulletin service provided to the UK Foreign, Commonwealth and Development Office (FCDO). This service was designed to provide on-demand bulletins that synthesise weather, hydrological, coastal surge and flood inundation information into a short report

https://doi.org/10.5194/egusphere-2025-3473
Preprint. Discussion started: 2 October 2025

format accessible to practitioners in FCDO and other partners. The service aimed to provide early warning support and advisories to FCDO to inform its decision-making on when to act, what actions to take and where to target. The bulletins and advisories aim to provide an overview of potential flood situations and to provide timely and accurate early warnings and flood forecasting services.

The approach taken is outlined by a set of standard operating procedures (SOP) as shown in Figure 1. The SOP begin with a trigger and activation process where a decision is made to initiate the bulletin production process. This is followed by a mixture of technical analysis of forecast data (more information provided in the Methods section), expert interpretation of results and synthesis into a 2-3 page bulletin that can be shared as a PDF or printed. A feedback process and post-event review is also included. This diagram reflects the partner organisations involved in creating the bulletin, however most of the technical data sets and analysis could be exchanged for equivalents available to other organisations. The forecast system covers potential flooding from the fluvial response to rainfall and along the coast from tropical cyclone-induced surge.

Previous research has investigated the performance of tropical cyclone track and intensity forecasts (Emmerton et al., 2020) and there has also been work examining the bulletin production process, end user needs and communication of such bulletins (Emerton et al., 2020; Speight et al., 2024). However, there is a lack of information on how forecasts of people directly affected (i.e. population exposure), as represented by boxes 4a to 7 in the SOP diagram (Figure 1), should be interpreted, and there is little evidence available to support the use and dissemination of such forecast analysis.

To address this information gap, we analyse the degradation of the inundation and population exposure forecasts with increasing forecast lead time and aim to provide insights that might help when balancing the demand for local-scale exposure information with uncertainty. Forecasts for Tropical Cyclone Freddy in March 2023 were chosen for a deeper analysis of inundation forecasts due to the availability of suitable satellite data on flood extents for validation. The forecast covered both fluvial and coastal flooding. However, the surge was forecast to be approximately 1m for Tropical Cyclone Freddy, which, when combined with the tide, only just exceeded the highest astronomical tide. As a result, the coastal flooding was expected to be localised rather than widespread, which has subsequently been supported by post-event observations. Therefore, the forecast validation henceforth concentrates on the forecast of fluvial flooding associated with Tropical Cyclone Freddy.

Our results are arranged into two sections. Firstly, an assessment of forecast lead times where we ask:

- How does forecast population exposure typically change with lead time for recent landfalling tropical cyclones in East Africa?
- What implications does this have for the identification of population exposure hotspots, particularly with respect to the degree of forecast spatial aggregation?

Secondly, we evaluate inundation and exposure forecasts for tropical cyclone Freddy given remotely sensed flood extents obtained from the operational UNOSAT and Copernicus services, where we ask:

- How similar are the population exposure and flood inundation forecasts between data sets?
- To what extent is this comparison problematic given uncertainties in peak flood timing and event duration?
- Are there obvious limitations of the forecasting approach that should be communicated to the end user?

The bulletins were shared with humanitarian partners and in-country organisations. Feedback from these was collated and used to summarise the usefulness and uniqueness of the inundation information. Ongoing challenges

https://doi.org/10.5194/egusphere-2025-3473
Preprint. Discussion started: 2 October 2025

and limitations associated with the current technical capability are highlighted in the discussion. The aim of this work is not to qualify total uncertainty, but rather to i) share experience of using the data in a quasi-operational context and ii) highlight some of the issues faced in practice that an end user should be aware of.

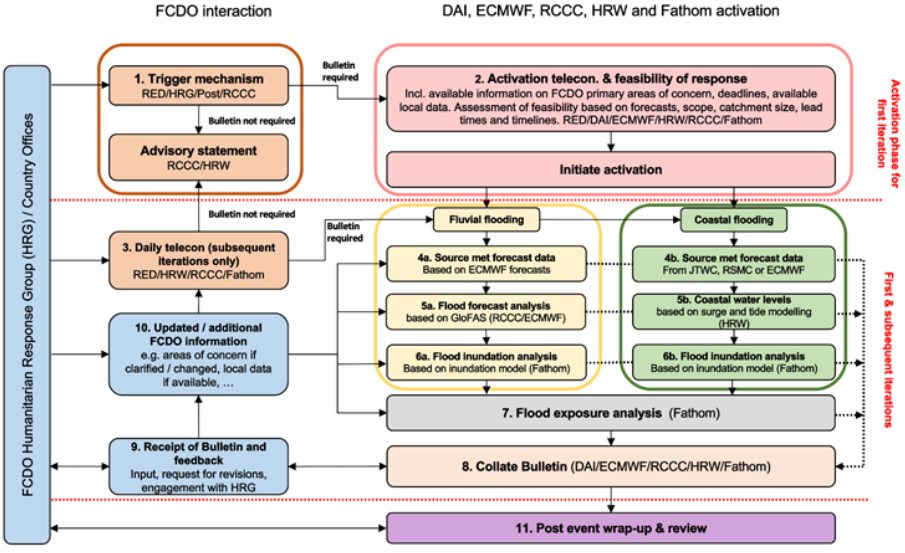

Figure 1: FCDO Pilot flood early warning standard operating procedures (October 2024 version)

2 Methods

We analysed forecasts of directly affected population (number of people flooded) and inundation extent from fluvial flooding for the five most recent landfalling tropical cyclones in East Africa and a total of seven landfalls. These are summarised in Table 1. Our method to forecast directly affected population (hereafter 'exposure') was based on four data sets that cascade into each other following steps 4a, 5a, 6a and 7 in Figure 1. Specifically:

2.1 European Centre for Medium Range Weather Forecast (ECMWF) weather forecasts (rainfall and storm track)

Weather forecasts were obtained from model cycle 47r3 of the ECMWF ensemble prediction system Owens, 2018; ECMWF, 2021). This system issues four weather forecasts per day, although only the forecasts produced at 00 UTC are input into the hydrological forecasting model. The ensemble forecasting system consists of a control member and 50 perturbed members that provide meteorological boundary conditions for the Global Flood Awareness System (GloFAS).

2.2 Global Flood Awareness System (GloFAS) forecasts (streamflow and streamflow return period)

GLoFAS versions 3.2 (for the 2022 events) and 3.4 (for the 2023 events) were used to provide forecasts of river streamflow. GloFAS is one component of the European Commission's Copernicus Emergency Management Service – Early Warning Service for Floods (CEMS-EWS Floods). GloFAS forecasts are published daily and are

https://doi.org/10.5194/egusphere-2025-3473
Preprint. Discussion started: 2 October 2025

used here for their accessibility, global coverage and because they anecdotally tend to be the most well-known system amongst humanitarian responders using the bulletins generated. Locally calibrated streamflow forecasting systems could likely outperform GloFAS in terms of river discharge prediction, especially if historical river gauge observations are available.

GloFAS is designed to simulate streamflow on large rivers globally using ensemble meteorological forecasts from ECMWF, which are input to the LISFLOOD open source hydrological model (van der Knijff et al., 2010), developed by the Joint Research Centre (JRC) of the European Commission. Note that the LISFLOOD hydrological model should not be confused with the LISFLOOD-FP flood inundation model used for inundation simulation in the next section.

Streamflow forecasts for 51-ensemble members were provided at 24 hour timesteps up to a maximum lead time of 30 days in every ~10 km grid cell where the upstream drainage area was ≥1000 km^2. Since Tropical Cyclone Freddy, a major upgrade to GloFAS (version 4.0) was released on the 23rd July 2023, this included reducing the spatial resolution 3 arcminutes (~5 km at the equator), more details are given in Matthews et al. (2025).

2.3 Fathom flood hazard maps (flood depth and extent by return period)

Flood depths and extents were obtained from the Fathom Global Flood Map version 3 (Wing et al., 2024). These data provide global flood hazard information at ~30m spatial resolution for 10 return periods from 5 to 1000 years. Flood inundation is simulated by the LISFLOOD-FP hydrodynamic model (Neal et al., 2012), taking as inputs elevation data from FABDEM (Hawker et al., 2022) and river discharges from a global flood frequency analysis (Smith et al., 2015). River locations are defined by the MERIT HYDRO river topology (Yamazaki et al., 2019), where river bathymetry is estimated using the methods of Neal et al. (2021). An overview of the modelling framework and data is provided by Wing et al. (2024) and Sampson et al. (2015), with additional validation provided by Hawker et al. (2024).

2.4 Surge forecast modelling

Coastal sea levels are modelled using the TELEMAC-2D hydrodynamic model (Hervouet, 2007) forced by wind and atmospheric pressure fields generated from tropical cyclone advisories issued by the designated Regional Specialised Meteorological Centre, in this case Meteo France on La Reunion. For Tropical Cyclone Freddy, the surge model covered the Mozambique channel and included tide as well as the cyclone-generated surge to provide projections of total water level. The surge modelling method is described in Grey et al. (2022) and Grey et al. (2024). Time and spatially varying water levels from TELEMAC-2D are then applied as boundary conditions to a LISFLOOD-FP model set up equivalent to those used in the Fathom Global Flood Map (Wing et al. 2024) to predict the extents of coastal inundation.**WorldPop population data (population counts)**

Population counts were based on WorldPop constrained data at 3 arc-second resolution (~100m), with population counts projected to the year 2020 (Bondarenko et al., 2020; Stevens et al., 2015). This version of WorldPop employs a random forest method to allocate census data from administrative units to specific building locations, utilising a range of spatial covariates. WorldPop constrained was chosen primarily for its resolution relative to other national and global population data sets available in the region and its constraint of population to buildings (Bondarenko et al., 2020). Both these factors are necessary to avoid flood exposure over-prediction bias of up to 40% which can occur when people are imprecisely located along the edge of floodplains (Smith et al., 2019).

https://doi.org/10.5194/egusphere-2025-3473
Preprint. Discussion started: 2 October 2025

However, there are known problems associated with these data for humanitarian applications. In Mozambique, the census data on which the population projections are based is dated from 2007 and WorldPop is known to underrepresent informal settlements (Thomson et al., 2021). Furthermore, the data do not account for in-country displacement, notably from Tropical Cyclone Idai and conflict in the country's northern districts where estimates of internal displacement exceeded 470,000 people in Mozambique (IDMC, 2019; Mester et al., 2023)

2.5 Forecast generation

Below is a concise outline of how the data sets are used and combined in the analysis chain. Our forecasts start with the 51-member ensemble weather forecasts from the ECMWF Integrated Forecast System (IFS) (Owens, 2018), which provides input to the Global Flood Awareness System (GloFAS). GloFAS versions 3.2 and 3.4 provided 30-day duration streamflow forecasts on a ~10km gridded river network for each of the 51 weather forecasts. The streamflow forecasts were converted into an estimate of the return period using parameters derived from Gumbel distributions fitted at every grid cell to annual maximum streamflow values extracted from version 3.1 of the GloFAS hydrological re-analysis (Zsoter et al., 2021)..

To calculate the number of people directly affected (exposed), we construct flood inundation forecasts and intersect these with high-resolution population data from WorldPop. Flood inundation can be simulated by hydrodynamic models. However, these are computationally expensive to run in real time for country wide domains. Therefore, we use a library of flood inundation simulations at 1 arc second resolution (~30m) from the Fathom Flood Map S3 (Wing et al., 2024) for different magnitudes of flood (10 return periods in total from 1 in 10 to 1 in 1000 years). The method is conceptually similar to that adopted for operational rapid flood risk assessment in Europe (Dottori et al., 2017). An example of the hazard mapping data is provided by Figure 2, which plots flood depth for the 1 in 500 year return period in blue intersected with population in red. This particular map was produced as part of a forecast on 10/03/2023 for the city of Quilemane in Mozambique, which is close to the second landfall of Tropical Cyclone Freddy. To construct a flood footprint for each of the 51 GloFAS forecasts, the flood return period simulated by GloFAS was downscaled onto the higher resolution Fathom flood map river network. Finally, each flood footprint is overlain on WorldPop gridded population density data to identify people flooded, with total direct flooded population summed at the district level using geopolitical boundaries. Georeferenced packages of administrative boundaries for Mozambique and surrounding countries were downloaded from GeoBoundaries.org. Figure 3 illustrates this for the 25th, 50th and 75th percentiles of the ensemble forecast for the region impacted by the second landfall of Tropical Cyclone Freddy.

Table 1: Summary of recent tropical cyclones include in this study.

Event name	Date	Landfall location	Countries for which Exposure calculated
Batsarai	06/02/2022	Nosy Varika, Madagascar	Madagascar
Emnati	23/02/2022	Vatomandry, Madagascar	Madagascar
Gombe	11/03/2022	Nampula, Mozambique	Mozambique, Malawi
Freddy	21/2/2023	Mananjary, Madagascar	Madagascar
	24/2/2023	Vilankulos, Mozambique	Mozambique

https://doi.org/10.5194/egusphere-2025-3473
Preprint. Discussion started: 2 October 2025

	11/3/2023	Quilemane, Mozambique	Mozambique, Malawi

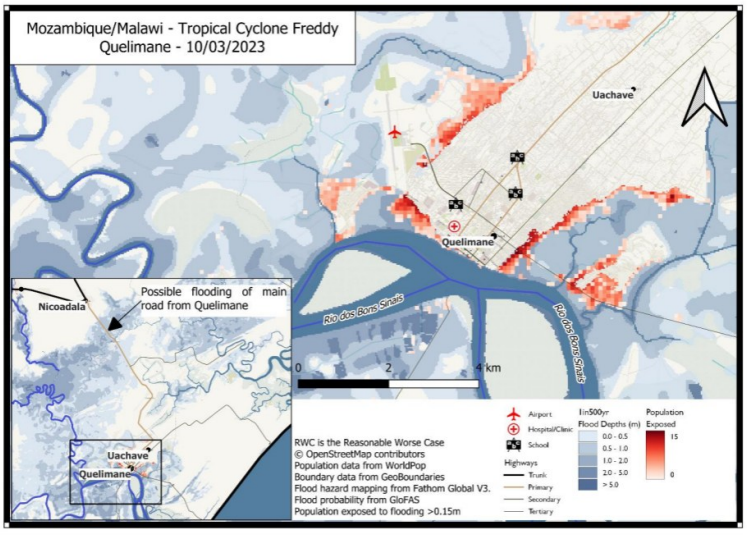

Figure 2: Maps illustrating flood hazard layers for the 1 in 500 year return period around Quelimane, Mozambique.

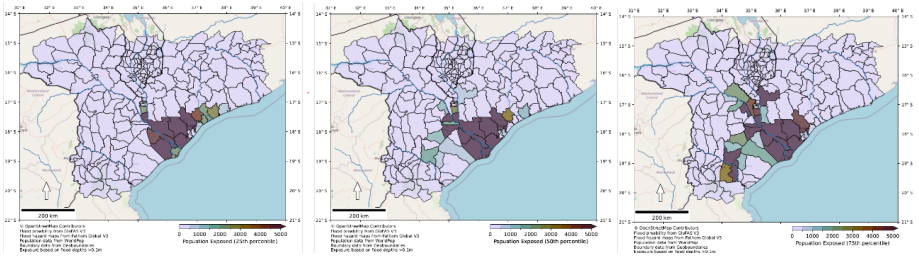

Figure 3: Maps of population exposure in Mozambique at district level for a tropical cyclone Freddy forecast, illustrating the 25th, 50th and 75th percentiles of the ensemble forecast exposure estimates.

3 Results

3.1 Assessment of forecast lead time

Our first analysis focuses on the evolution of the forecast population flooded (exposure) and the location of the exposure, when aggregated to the district administrative unit level, with lead time (note that districts are of different sizes depending on the country). The results of this analysis are plotted in Figure 4, where direct exposure to flooding is plotted each day from up to five days before landfall (sometimes only four days if no flooding is forecast) to one day after landfall. We stop one day after landfall under the assumption that satellite imagery of the flooding is more likely to be used post-event. The top row of bar plots indicates the total population flooded (exposure) for each of the 51 ensemble members. Almost all forecasts include some ensemble members with zero or near-zero flooding, except after landfall, where reanalysis rainfall data starts to dominate the forecast peaks and reduce the forecast spread. When interpreting this reduction in uncertainty, it is important to be aware that although the reanalysis rainfall is likely to be more accurate than the forecasted rainfall, the uncertainty reduction after

https://doi.org/10.5194/egusphere-2025-3473
Preprint. Discussion started: 2 October 2025

landfall is also due to the loss of ensemble spread in the rainfall inputs. The exposure distribution also tends to include outliers on the high side, with exposure as much as 10 times greater than the ensemble median often forecast by a few members. These outliers are typically driven by ensemble members that cause flooding over areas of high population, rather than being ensemble members with exceptionally intense rainfalls. Track location is therefore critical for exposure estimates even when aggregated to the district level. Reassuringly, for most tropical cyclones, the ensemble spread narrows as the lead time decreases, with the distribution of exposure forecast at or after landfall sitting within the spread of earlier forecasts. The exception is the second landfall of Tropical Cyclone Freddy, where the forecast only concentrates sufficiently one day prior to landfall.

Except for the second landfall of Tropical Cyclone Freddy, the median exposure tends to remain in the same order of magnitude across the lead times analysed here. In our experience, early use of the forecast exposure 3-5 days before landfall tends to be too uncertain in absolute numbers and location to be of much practical use, and a user of these forecasts needs an understanding of ensemble forecast uncertainty to interpret the results. Nevertheless, the forecasts tend not to be misinformative and thus appear useful to support anticipatory action, especially for no/limited regret actions, with the strong caveat that we expect substantial additional uncertainties from the inundation simulation and population data that are not captured by the ensemble forecasts and will persist regardless of forecast return period and lead-time.

Feedback from practitioners, mostly based at national and international organisations in this case, often highlights how identifying the most exposed locations (typically at district level) is particularly useful. Therefore, we are interested in how consistent the most exposed locations are with forecast lead time. The lower plots on Figure 4 show the population exposed by district (ensemble mean), highlighting the top five most exposed districts one day after landfall with a unique colour that is consistent with lead time. The sum of exposure in all other districts is then added to the bar in light blue. Thus, growth in the size of the blue bar with lead time indicates a reduction in focus on the five most exposed districts after landfall. Before interpreting these plots, it is worth considering a few aspects of the data. In these plots, the ensemble mean is used to indicate how exposed a district is, and this number is usually dominated by: a) the number of ensemble members that forecast flooding in that district; and b) the population living on the floodplain. We also see that the ensemble mean exposure typically increases and focuses on a few districts at shorter lead times. This was expected because all our events are landfalling tropical cyclones, meaning that the ensemble spread is decreasing and focusing over the land. We expect the opposite trend from tropical cyclones that have a near-miss landfall, but we do not include them in our analysis. As expected, the proportion of the exposure outside of the top five most exposed districts tends to increase with lead time due to the greater ensemble spread. Perhaps unsurprisingly, the extent to which the top five most exposed districts can be identified at longer lead times depends on the size of the districts. Districts in Mozambique and Malawi tend to be larger than those in Madagascar, meaning the predictions aggregated at the district level appear more stable. In Mozambique and Malawi, the top five most exposed districts usually account for over 50% of the exposure in the forecast one day after landfall, suggesting that the footprint of the cyclone's most intense impact doesn't tend to extend significantly beyond five districts. It is also worth noting that urban areas exposed to flooding tend to dominate and a different set of metrics would be needed to assess exposure in rural communities. For example, in the Fathom flood hazard data, the population exposed to flooding in urban areas along the Limpopo river (e.g. Chockwe, Xai-Xai) at almost any return period exceeds the population exposed to the greatest return period in sparsely populated districts directly north.

https://doi.org/10.5194/egusphere-2025-3473
Preprint. Discussion started: 2 October 2025

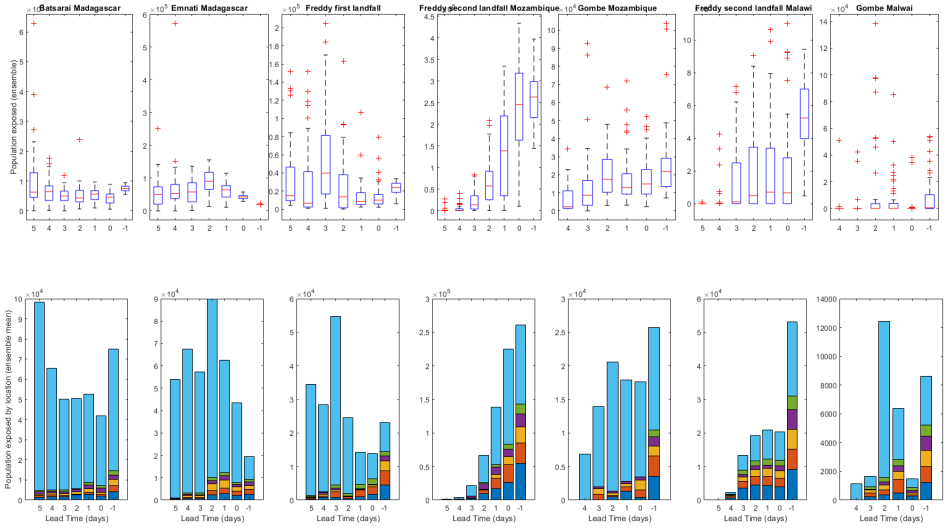

Figure 4: Ensemble spread of exposure forecasts with lead time for five land falling tropical cyclones in Mozambique, Malawi and Madagascar (top plot) and ensemble mean exposure disaggregated by district to the five most exposed districts as forecast one day after landfall (lower plot). The top 5 most exposed districts are identified by differently coloured stacked bars, with all other districts plotted on top as a single colour (lighter blue)

Focusing on the case of Tropical Cyclone Freddy from five to two days before its first landfall in Mozambique can help illustrate the observations above. Figure 5 plots observed (RSMC analysis) and forecasted (ECMWF) track position of Freddy and the probability of precipitation accumulations in the next five days exceeding 200 mm according to the ECMWF ensemble forecast. Plots relate to the first landfall of Freddy on the a) 22nd b) 23rd c) 30th February and for the second landfall of Freddy on the d) 9th e) 10th and f) 13th March 2023. These days correspond to when bulletin updates were issued by the team.

The low probabilities shown on the 22nd in Figure 5*a* are the result of uncertainty in the location of the heavy rainfall. This figure should be interpreted as showing the area (shown by the shading) within which heavy rainfall between 200-400mm (and up to 800-1000mm in places) is possible. This uncertainty is evident in the exposure forecasts in Figure 4, which range from close to zero to almost 200k people flooded. Especially high exposures, for example, three days before landfall, were caused by some ensemble members forecasting heavy rainfall south of the Limpopo River to areas of the Incomati River that had flooded earlier in the month and the Maputo area (capital city of Mozambique). These low-probability but high-impact forecasts were a significant concern due to potential impacts on important national infrastructure. We speculate that risk characterisation storylines and worst case narratives may be useful or desired by end users to capture low probability but potentially catastrophic impacts. However, in this case, focusing on the worst case scenarios would have completely missed the impacted location.

From 1-2 days before landfall, heavy rainfall as far south as the Maputo area was no longer being forecast, substantially reducing the worst case exposure estimates. Forecast exposure for Freddy's first landfall was usually dominated by flooding along the Limpopo river (close to the forecast control member track), including population

https://doi.org/10.5194/egusphere-2025-3473
Preprint. Discussion started: 2 October 2025

centres around Chókwè where a ~1 in 20 year return period flood was forecast by some ensemble members. By the day after landfall (Figure 5*c*) the heaviest rainfall strengthens but shifts northwards into a region of sparser population where few settlements are on floodplains.

Focusing on the second landfall of Freddy, substantial uncertainty in the forecast track results in little exposure being forecast 3-5 days before landfall. However, by the 9th March (2 days before landfall) the forecast is more organised. Figure 5*d* illustrates the ECMWF forecast on this day and indicates that Tropical Cyclone Freddy is expected to bring heavy rainfall to Zambezia, Tete and Manica districts, and is expected to move inland to also affect northern Sofala district and southern Malawi (details of these locations are covered in the next section). Cumulative rainfall totals between 150-300mm are expected in these areas, whilst totals between 500-800mm are possible in some areas, but their location is uncertain. These uncertainties are reflected in the forecast exposure two days before landfall, which subsequently reduces and focuses on greater exposure one day prior to landfall (Figure 5*e*). The mean location of the forecast tracks did not change much from two days out, meaning the top five most exposed locations remain reasonably consistent (Figure 4).

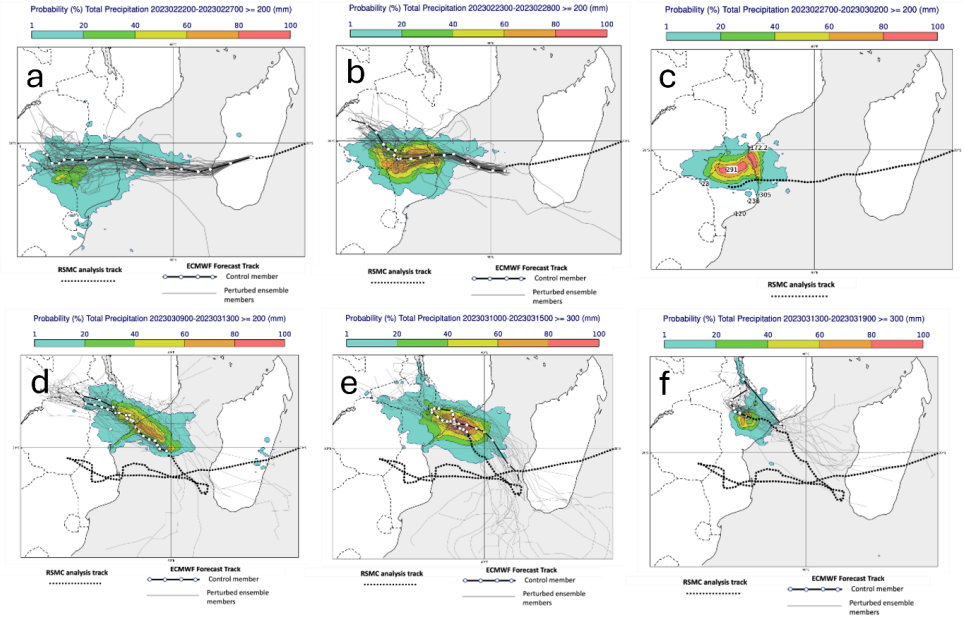

Figure 5: Observed (RSMC analysis) and forecasted (ECMWF) track position of Freddy and the probability of precipitation accumulations in the next 5 days exceeding 200 mm according to the ECMWF ensemble forecast. Plots relate to the first landfall of Freddy on the a) 22nd b) 23rd c) 30th February and for the second landfall of Freddy on the d) 9th e) 10th and f) 13th March 2023.

3.2 Comparison of inundation forecasts with remotely sensed flood extents

This section provides some indicative information on relative forecast skill that might be useful for an end user of the forecast data, and discusses some of the limitations and challenges of the evaluation. Inundation and exposure forecasts made for the second landfall of Tropical Cyclone Freddy were compared to open-source post-event remote sensing, which is widely used during post-disaster response. When obtaining remotely sensed data, we only use flood extents provided via Copernicus and UNOSAT as part of their disaster response. In total, eight

https://doi.org/10.5194/egusphere-2025-3473
Preprint. Discussion started: 2 October 2025

remotely sensed images are considered (see Table 2), captured over the period 14th-17th of March 2023, with most locations imaged twice over this period. Some later observations are also available (listed at the end of Table 2) via these services, however we do not consider them because the flooding has receded from earlier scenes. We assume all remotely sensed flood extents are equal and do not assess their accuracy. However, we note that the images are unlikely to be coincident with peak flooding and, as Synthetic Aperture Radar (SAR) derived products, they will not detect flooding in urban and vegetated areas (Shen et al., 2019). The derived flood extents are mapped in Figures S1 to S28 in the Supplementary Data section, with most locations mapped multiple times, as this captured more flooding on larger rivers where flood wave propagation could take several days. Exposure data for both the forecasts and remotely sensed data are aggregated to the district level for the analysis, with the districts plotted in Figure 6. Some flooding that is potentially pluvial in origin (e.g. not from a river going out of bank) can be seen around Quelimane on the 14th. However, in general the remote sensing is likely to have missed substantial pluvial and flash flooding on smaller rivers, some of which may be simulated by the Fathom inundation model if the catchment is larger than approximately 50km^2. Therefore, we believe it is reasonable to assume the remote sensing is a conservative estimate of the actual maximum flood extents and we present this work as a comparison rather than a validation of either method due to the expectations that an exact match in exposure is not expected. We note that forecast skill is likely to change substantially depending on the geography of the region being impacted, meaning the results below are not transferable between locations and should be interpreted as merely indicative of forecast skill.

Table 2: Summary of remotely sensed data used for validation

Source	ID	Location	Data	Time UTC	Sensor	Inundation maps
UNOSAT	3528	Sofala and Zambezia Provinces	14/03/2023	3:10	RADARSAT[1]	S1-S4
UNOSAT	3529	Southern Malawi	14/03/2023	3:10	RADARSAT[1]	S5-S8
Copernicus	EMSR654	Quelimane Release 1	14/03/2023	14:47	COSMO-SkyMed[2]	S9-S12
Copernicus	EMSR654	Mutarara Release 1	15/03/2023	3:53	COSMO-SkyMed[2]	S13-S15
Copernicus	EMSR654	Mutarara Monitoring 1	16/03/2023	3:09	RADARSAT[3]	-
UNOSAT	3529	Southern Malawi	17/03/2023	3:03	Sentinel 1[4]	S16-S20
UNOSAT	3528	Sofala and Zambezia Provinces	17/03/2023	3:03	Sentinel 1[4]	S21-S24
Copernicus	EMSR654	Quelimane Monitoring 1	17/03/2023	14:53	COSMO-SkyMed[2]	S25-S27

https://doi.org/10.5194/egusphere-2025-3473
Preprint. Discussion started: 2 October 2025

Copernicus	EMSR654	Mutarara Monitoring 1	16/03/2023	3:05	RADARSAT[3]	
Additional data was published for the following events, however all either only showed reduced flooding from the earlier imagery, or were superseded by a further update that is covered in more detail. Specifically: UNOSAT 3543 Southern Region, Malawi. Situation at 21/03/2023 UNOSAT 3541 Sofala and Zambezia Provinces. Situation at 21/03/2023 at 07:55 UTC Copernicus EMSR654 Quelimane Monitoring 2. Situation at 22/03/2023 at 14:47 UTC Copernicus EMSR654 Mutarara Monitoring 2. Situation at 17/03/2023 at 03:09 UTC						

1. RADARSAT Constellation Mission Imagery © Government of Canada (2023)
2. COSMO-SkyMed© ASI (2023), distributed by e-GEOS S.p.A.
3. RADARSAT 2 Data and products © Mac Donald, Dettwiler and Associates Ltd.
4. Sentinel 1 - Contains modified Copernicus Sentinel data

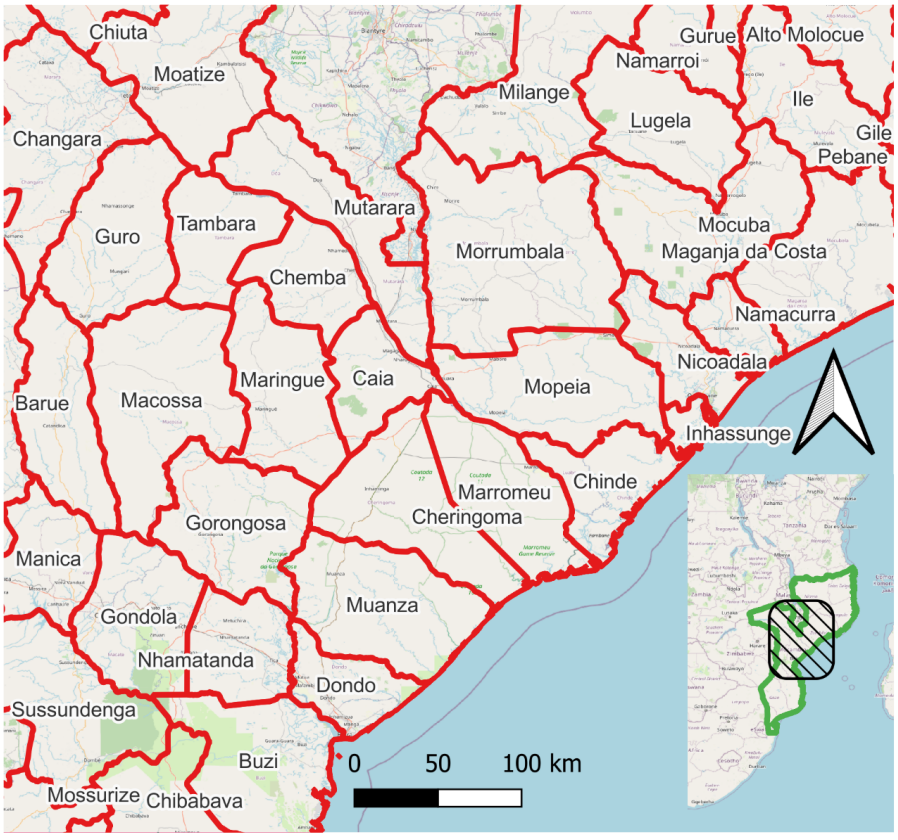

Figure 6: Map of the districts in Mozambique considered in this section. Open data sourced from GeoBoundaries and ©OpenStreetMap.

Population exposure, given the remote sensing data, was calculated from the same WorldPop layer used to forecast exposure. Population exposure to each image is summarised in supplementary tables S1 to S8 for each district within the images, along with the total population in each district according to WorldPop. Table 3 summarises the

https://doi.org/10.5194/egusphere-2025-3473
Preprint. Discussion started: 2 October 2025

population exposure for each district where exposure is above 1000 people, using the maximum of the remotely sensed flood extents where multiple images are available. The forecast model comparison against each image is discussed in more detail in the supplementary validation section, and we draw on this more detailed discussion when making some conclusions.

Given the substantial uncertainty in the forecast return period, we compare the inundation and exposure predictions for eight return periods between 1 in 5 year and 1 in 1000 year (see Supplementary Tables S1-S8). However, we also highlight the best estimate from the forecast ensemble (median return period) and a reasonable worst case (highest return period from the ensemble) and report these exposures in Table 3. We have not computed fit statistics between the remotely sensed flood extents and the model flood extents, which often compare the area of agreement between two flood extent data sources to areas of over- and under-prediction using metrics such as the F-statistic and critical success index (Landwehr et al., 2024). A visual analysis of the difference between the data sets suggests such an analysis would be complicated to interpret because apparent over-prediction by the model often occurs over low-lying areas close to the rivers where vegetation is likely obscuring the remotely sensed flood extents and there is little or no population. Instead, the analysis will qualitatively discuss the inundation extent and use population exposure as the primary quantitative measure of agreement between the data sets, which is likely of more interest in the early stages of a disaster than inundation extent. The timing of the inundation arrival or peak has not been considered in our forecasts because we do not have a good way to evaluate flood arrival time, although there is evidence from the multiple images that flood extents are dynamic over the observation period and, in some cases, increase between images. Suggesting that the remotely sensed images may miss some flooding due to temporal sampling.

Overall exposure estimates are remarkably similar between the remotely sensed flood extents and the best estimate from the forecast, with 126k people flooded in the remote sensing and 171k flooded by the forecast model best estimate (Total exposure at the end of Table 3). This 26% difference is even smaller at 21% when only districts with over 1000 people flooded are considered (in general, we might expect small-scale flooding to be more difficult to simulate with the inundation model and more sensitive to GloFAS return period errors). However, this overall similarity averages substantially greater differences at the district scale. The three most exposed districts have differences below 30%, however the 4th most exposed district (Phalombe in Malawi) is not captured by the best estimate and the reasonable worst case scenario presented in Table 3. GloFAS does not forecast flooding this far north in any ensemble member. However, the flood hazard layers can simulate the observed flooding (See Supplementary figure S5 and table S2) and would have returned exposure had GloFAS forecast the flooding. Exposure is greater in the forecast for the fifth most exposed district (Nsanje) where exposure is relatively sensitive to return period compared to other locations (See Tables S2 and S8), and a 1 in 5 year return period forecast would have returned values similar to the remote sensing. Note that the remote sensing may also underestimate in urban and vegetated areas because the water surface is obscured from the sensor by surface artefacts (e.g. vegetation and buildings) (Shen et al., 2019). Underprediction by the forecast model is also seen, for example in Mulanje, where greater return periods than the best estimate are a closer match to the remote sensing.

https://doi.org/10.5194/egusphere-2025-3473
Preprint. Discussion started: 2 October 2025

Table 3: Summary of exposure estimates from remotely sensed data and GloFAS forecast on the day of landfall by district. From left to right showing the district name, best estimate (BE) return period from GloFAS, reasonable worst case scenario (RWC) from GloFAS, Population exposure to remote sensing data (taking the maximum over all images), and forecast population exposure given GloFAS return period and Fathom flood hazard layer. Forecast return period is not reported if below 1 in 5 year.

District Name	Return period estimated from GloFAS		Max exposure from observed extents	Population exposure from combined GloFAS return period and flood hazard layer			
	BE	**RWC**		**BE**	**Diff %**	**RWC**	**Diff %**
Mutarara	1in200	1in500	19353	26773	-27%	28073	-31%
Morrumbala	1in200	1in500	16380	15787	3.8%	18663	-12%
Nicoadala	1in500	1in1000	15361	15391	-0.19%	18462	-16%
Phalombe			14938	0		0	
Nsanje	1in200	1in500	8625	18303	-53%	20075	-57%
Namacurra - Namacurra	1in500	1in1000	6830	4406	55%	4947	38%
Mulanje	1in20	1in50	5599	919	509%	1427	292%
Inhassunge	1in500	1in1000	4922	733	571%	807	509%
Milange - Rio Shire	1in20	1in50	4860	1117	334%	1625	199%
Cidade De Quelimane	1in500	1in1000	4243	33439	-87%	36871	-88%
Chikwawa	1in20	1in50	4144	25727	-83%	31613	-86%
Maquival	1in500	1in1000	3952	614	543%	770	413%
Zomba			3703	0		0	
Maganja Da Costa	1in200	1in500	3190	4987	-36%	6698	-52%
Chinde			1950	0		0	
Namacurra - Rio Lucungo	1in200	1in500	1714	3375	-49%	4484	-61%
Mopeia	1in500	1in1000	1522	3069	-50%	3304	-53%
Total			121286	154640	-21%	177819	-31%
Other (<1000 exposed)[1]			4926	16837	-241%	17558	-256%
Total			126213	171477	-26%	195377	-35%

1. Other (exposure below 1000) are: Mopeia - Zambezi Region, Caia - Zambezi Region, Caia - Not Zambezi, Molumbo - Zambezi Region, Chiradzulu, Thyolo, Luabo, Mutarara - Zambezi Region, Mocubela, Doa - Zambezi Region, Chemba - Zambezi Region, Marromeu - Zambezi Region, Cheringoma - Inland Reg, Blantyre, Doa - Not Zambezi, Muanza - Coastal Region, Pebane, Mocuba - Rio Licungo, Cheringoma - Coastal Re, Derre

4 Discussion and conclusions

Here we attempt to synthesise the results above into a set of plain language statements about the exposure forecasts that aim to be a useful starting point for interpreting the outputs in a practical setting. This is organised by initially presenting some general observations before breaking down using our five research questions.

Firstly, it is misleading not to consider the ensemble - uncertainty dominates the messaging in all forecasts even after landfall. Low probability but high impact ensemble members are seen in most forecasts, along with ensemble

https://doi.org/10.5194/egusphere-2025-3473
Preprint. Discussion started: 2 October 2025

members that indicate little or no flooding of people. Despite the importance of uncertainty, a key limitation of the methods used here is that the ensemble only considers uncertainty in the rainfall from the ECMWF forecast ensemble. Other sources of uncertainty, especially in the population data, hydrological modelling and inundation extents, are likely to be important and may generate biases irrespective of lead time and the forecast.

The first half of the results set out to describe how the forecast exposure typically changed with lead time for recent landfalling tropical cyclones in East Africa, and the implications of this for the identification of exposure hotspots, particularly with respect to the degree of forecast spatial aggregation.

How does forecast exposure typically change with lead time for recent landfalling tropical cyclones in East Africa?

The number of people forecast to be flooded and their location could change substantially with lead time. Therefore, the number of people exposed and the locations of the exposure should probably not be disseminated to untrained users for forecasts with lead times greater than 2 days. However, the information might be useful to expert forecasters if considered in the context of past forecasts. With the number of forecasts analysed here, it is not possible to qualitatively analyse forecast skill, however most of the forecasts we analysed were informative in that range of forecast exposures bracketed the day after landfall forecast exposure. The exception is the second landfall of Freddy, where the exposure grows rapidly as the forecast date moves closer to landfall, with early forecasts (2-5 days ahead) substantially underestimating exposure. Forecasters should consider the possibility that exposure forecasts could be misinformative. This discussion was often undertaken by the forecast team during a daily telecon (Steps 2 and 3 in Figure 1) and relied on expert judgement from the meteorological forecasters and often some comparison with other forecast centres. For example, if the UK Met Office or US Global Forecasting System had different track predictions, the possibility of forecast bias or substantial error often delayed the decision to issue a bulletin until there was greater confidence.

What implications does lead time have for the identification of exposure hotspots, particularly with respect to the degree of forecast spatial aggregation?

The decision to make a forecast of the most impacted locations was intrinsically linked to the degree of aggregation in specifying that location, e.g. it's possible to specify the most exposed locations but there needed to be a suitable levels of spatial aggregation for this to be reliable. Districts in Mozambique and Malawi were large enough to identify the majority of the most exposed districts 1-2 days before landfall for the events we have analysed. However, the smaller districts in Madagascar meant that the aggregated exposures tended to change substantially right up to landfall. Drilling down further to individual towns and cities will add further uncertainty, however as a few urban areas tended to dominate the exposure estimates the exposure forecast for individual cities often looks very similar to the district level exposure estimates in terms of most exposed locations. We found that a degree of expert judgement and interaction with the stakeholders was needed to decide on the level of forecast aggregation, and insights from meteorologists regarding the storm track were also crucial. Exposure hotspots were dominated by urban areas on floodplains, which could be identified by the hazard mapping in advance of making forecasts, as a precursor to responding to an event.

The second half of our results compared exposure and inundation forecasts to estimates from open-source remote sensing data, discussed some challenges with comparing the data sources and highlighted some principal limitations of the forecasting approach. Overall, our comparison between the remote sensing and forecast

https://doi.org/10.5194/egusphere-2025-3473
Preprint. Discussion started: 2 October 2025

inundation shows a hugely complex set of results, with a more complete description of that complexity provided in the supplement.

How similar are the exposure and inundation forecasts between data sets?

The forecast model can both over- and under-predict the observed flooding given by remote sensing at the district scale. However, the overall spatially aggregated exposure estimates are surprisingly similar. Forecast exposure mapping could perform well against remote sensing, but substantial uncertainty over forecast return period (likely in GloFAS and the inundation model) means that the return period forecast was rarely an accurate match to the remote sensing. However, the remotely sensed exposure usually sat within the range of the return periods simulated by the hazard model. Attempting to forecast return period and associated exposure was therefore spuriously precise for the event we analysed. However identifying the most exposed districts and the range of exposures that might occur in those was able to yield exposure information that was consistent with the post landfall remote sensing, although our analysis of lead time suggests that this was only possible 1-2 days before landfall for the event we have analysed.

To what extent is this comparison problematic given uncertainties in peak flood timing and event duration?

Making a like-for-like comparison of the inundation modelling and remote sensing was highly problematic in this context because the inundation event is not simulated dynamically. Remote sensing shortly after landfall showed evidence of flooding in areas the flood model considers as pluvial flooding (technically catchments with <6 hours time to concentration or < 50km^2) and we also expect these images to include locations where the flooding has already occurred and receded, and locations yet to flood given the large scale nature of the analysis. Remote sensing is widely used for post landfall flood detection, however our results suggest that a combined approach considering both forecast and observed inundation extents might be useful. This would aim to fill gaps in the remotely sensed data, especially in urban and vegetated areas, and where flooding has receded on smaller reaches. Similarly, the return periods estimated from the inundation model and GloFAS were highly uncertain and matching of the inundation model data to remote sensing might substantially reduce uncertainty or rule out some ensemble members.

Are there obvious limitations of the forecasting approach that should be communicated to the end user?

Our inundation forecasting method can break down at confluences of large rivers where the water level response to the tropical cyclone is less extreme than that on smaller tributaries, the Zambezi being particularly obvious in this case. Independent simulations of the river flooding on the main river and its tributaries, or a fully dynamic simulation of river flows from each ensemble member that captures river-river compounding effects, are needed. A simple hazard map lookup system, as used here, should be expected to perform poorly where there is substantial compounding between a large river and its tributaries, regardless of the skill of GloFAS on individual rivers. One solution would be to implement a dynamic model run of the inundation model. However, this is difficult because dynamic simulations would need to be run for each (or many) ensemble members to capture the forecast uncertainty from GloFAS. This may i) prove to be computationally expensive if 30m resolution is maintained, and ii) be difficult to implement operationally because robust code is needed to run in real time along with reliable access to computing resources.

Practical considerations are especially relevant when the forecasting method is considered in a humanitarian context. The fluvial forecasting approach used here requires no real-time computing and, if well organised, could be designed to run on a standard desktop machine. If population exposure at districts is the key output, a lookup

https://doi.org/10.5194/egusphere-2025-3473
Preprint. Discussion started: 2 October 2025

table approach could even be used with the GloFAS web portal. Taking a dynamic approach to the simulations likely requires an operational forecasting centre to adopt and maintain the inundation modelling component. We know of no operational global inundation model that forecasts with the resolution used here at this time.

Data availability

All data used in this paper are openly accessible. GloFAS data are available from the Copernicus Climate Data Store https://cds.climate.copernicus.eu/. Fathom flood hazard data for Mozambique, Malawi and Madagascar are available from the University of Bristol Research Data Storage Facility under DOI https://doi.org/10.5523/bris.1kwwzgckmkx0u1ziflno3fgba9. Population data from WorldPop are available at https://www.worldpop.org/.

Author contributions

JN prepared the manuscript with contributions from all co-authors. AC undertook the remote sensing analysis. SC, LH and AC coded the linking of GloFAS and the Fathom flood hazard layers. SG and JS simulated coastal flooding. CB provided GloFAS data and interpreted the meteorological data. All authors interpreted forecasts and were involved in the bulletin production process.

Competing Interests

The authors declare that they have no conflict of interest.

Acknowledgements

This work was funded by the FCDO flood early warning pilot and additionally supported by NERC under grant NE/S015795/1 and FCDO via the CLARE project REPRESA.

References

Alfieri, L., Salamon, P., Bianchi, A., Neal, J., Bates, P. D., and Feyen, L. (2014) Advances in pan-European flood hazard mapping, Hydrol. Process., 28, 4928–4937, https://doi.org/10.1002/hyp.9947

Bondarenko, M., Kerr, D., Sorichetta, A., Tatem, A., and WorldPop: Census/projection-disaggregated gridded population datasets for 51 countries across sub-Saharan Africa in 2020 using building footprints, University Of Southampton [data set], https://doi.org/10.5258/SOTON/WP00682, 2020.

Dottori, F., Kalas, M., Salamon, P., Bianchi, A., Alfieri, L., and Feyen, L. (2017) An operational procedure for rapid flood risk assessment in Europe, Nat. Hazards Earth Syst. Sci., 17, 1111–1126, https://doi.org/10.5194/nhess-17-1111-2017

ECMWF (2021) IFS Documentation CY47R3 - Part V Ensemble prediction system. https://doi.org/10.21957/zw5j5zdz5

Emerton, R., Cloke, H., Ficchi, A., Hawker, L., de Wit, S., Speight, L., Prudhomme, C., Rundell, P., West, R., Neal, J., Cuna, J., Harrigan, S., Titley, H., Magnusson, L., Pappenberger, F., Klingaman, N., Stephens, E. (2020) Emergency flood bulletins for Cyclones Idai and Kenneth : A critical evaluation of the use of global flood forecasts for international humanitarian preparedness and response. *International Journal of Disaster Risk Reduction*. Vol. 50. https://doi.org/10.1016/j.ijdrr.2020.101811

https://doi.org/10.5194/egusphere-2025-3473
Preprint. Discussion started: 2 October 2025

Grey, S., Day, K., & Turnbull, M. (2022). Forecasting tropical cyclone surge. Proceedings of the XXVIIIth TELEMAC User Conference, 115–122.

Grey, S., Turnbull, M. and Simmons, J., 2025. Hurricane surge and inundation in the Bahamas, part 1: Storm surge model. *Journal of Flood Risk Management*, *18*(1), p.e13018. https://doi.org/10.1111/jfr3.13018

Hawker, L., Neal, J., Savage, J., Kirkpatrick, T., Lord, R., Zylberberg, Y., Groeger, A., Thuy, T. D., Fox, S., Agyemang, F., and Nam, P. K. (2024) Assessing LISFLOOD-FP with the next-generation digital elevation model FABDEM using household survey and remote sensing data in the Central Highlands of Vietnam, Nat. Hazards Earth Syst. Sci., 24, 539–566, https://doi.org/10.5194/nhess-24-539-2024

Hawker, L., Uhe, P., Paulo, L., Sosa, J., Savage, J., Sampson, C., & Neal, J. (2022). A 30 m global map of elevation with forests and buildings removed. *Environmental Research Letters*, **17**(2), 024016. **https://doi.org/10.1088/1748-9326/ac4d4f**

Hervouet, J. M. (2007). Hydrodynamics of Free Surface Flows: Modelling with the finite element method, Hydrodynamics of Free Surface Flows: Modelling with the finite element method. John Wiley and Sons. https://doi.org/10.1002/9780470319628

Internal Displacement Monitoring Centre (IDMC) (2019) Tropical Cyclone Idai. IDMC. Rue de Varembé 3, 1202 Geneva, Switzerland. GRID-2019-Disasters-Figure-Analysis-Idai.pdf (accessed July 2025)

Lu, D., Ding, R., Mao, J., Zhong, Q., & Zou, Q. (2024). Comparison of different global ensemble prediction systems for tropical cyclone intensity forecasting. *Atmospheric Science Letters*, 25(4), e1207. https://doi.org/10.1002/asl.1207

Mathews, G., Baugh, C., Barnard, C., Carton De Wiart, C., Colonese, J., Grimaldi, S., Ham, D., Hansford, E., Harrigan, S., Heiselberg, S., Hooker, H., Hossain, S., Mazzetti, C., Milano, L., Moschini, F., O'Regan, K., Pappenberger, F., Pfister, D., Man Rajbhandari, R., Salamon, P., Ramos, A., Shelton, K., Stephens, E., Tasev, D., Turner, M., van den Homberg, M., Wittig, J., Zsótér, E., Prudhomme, C. (2025) Chapter 15 - On the operational implementation of the Global Flood Awareness System (GloFAS) in Flood Forecasting (Second Edition). Eds Thomas E. Adams, Chandana Gangodagamage, Thomas C. Pagano. https://doi.org/10.1016/B978-0-443-14009-9.00014-6.

Mester, B., Vogt, T., Bryant, S., Otto, C., Frieler, K., and Schewe, J. (2023) Human displacements from Tropical Cyclone Idai attributable to climate change, Nat. Hazards Earth Syst. Sci., 23, 3467–3485, https://doi.org/10.5194/nhess-23-3467-2023.

Nauman, C., Anderson, E., Coughlan de Perez, E., Kruczkiewicz, A., McClain, S., Markert, A., Griffin, R., & Suarez, P. (2021). Perspectives on flood forecast-based early action and opportunities for Earth observations. *Journal of Applied Remote Sensing*, **15**(3), 032002. https://doi.org/10.1117/1.JRS.15.032002

Neal, J., Hawker, L., Savage, J., Durand, M., Bates, P., & Sampson, C. (2021). Estimating river channel bathymetry in large scale flood inundation models. *Water Resources Research*, **57**(5), e2020WR028301. **https://doi.org/10.1029/2020WR028301**

Neal, J., Schumann, G., & Bates, P. (2012). A subgrid channel model for simulating river hydraulics and floodplain inundation over large and data sparse areas. *Water Resources Research*, **48**(11), W11506. **https://doi.org/10.1029/2012WR012514**

UN OCHA, Cyclones Idai and Kenneth. Southern and Eastern Africa (ROSEA). https://www.unocha.org/southern-and-eastern-africa-rosea/cyclones-idai-and-kenneth

https://doi.org/10.5194/egusphere-2025-3473
Preprint. Discussion started: 2 October 2025

Owens, R G, Hewson, T D (2018). ECMWF Forecast User Guide. Reading: ECMWF. doi: 10.21957/m1cs7h

Shen, X., Anagnostou, E. N., Allen, G. H., Brakenridge, R. and Kettner, A. J. (2019) Near-real-time non-obstructed flood inundation mapping using synthetic aperture radar, *Remote Sensing of Environment*, **221**, https://doi.org/10.1016/j.rse.2018.11.008.

Smith, A., Bates, P., Wing, O., Sampson, C., Quinn, N., Neal, J. (2019) New estimates of flood exposure in developing countries using high-resolution population data, *Nature Communications*, https://doi.org/10.1038/s41467-019-09282-y

Smith, A., Sampson, C., & Bates, P. (2015). Regional flood frequency analysis at the global scale. *Water Resources Research*, **51**(1), 539–553. **https://doi.org/10.1002/2014WR015814**

Speight, L., Stephens, E., Hawker, L., Baugh, C., Neal, J., Cloke, H., Grey, S., Titley, H., Marsden, K., Sumner, T., Ficchi, A., Prudhomme, C., Archer, L., Bazo, J., Dambo, J., Dolan, S., Huhn, A. L., Moschini, F., Savage, J., Wanzala, M. (2023). Recommendations to improve the interpretation of global flood forecasts to support international humanitarian operations for tropical cyclones. Journal of Flood Risk Management, e12952. https://doi.org/10.1111/jfr3.12952

Stevens FR, Gaughan AE, Linard C, Tatem AJ (2015) Disaggregating Census Data for Population Mapping Using Random Forests with Remotely-Sensed and Ancillary Data. PLoS ONE 10(2): e0107042. https://doi.org/10.1371/journal.pone.0107042

Thomson, Dana R., Andrea E. Gaughan, Forrest R. Stevens, Gregory Yetman, Peter Elias, and Robert Chen. 2021. "Evaluating the Accuracy of Gridded Population Estimates in Slums: A Case Study in Nigeria and Kenya" *Urban Science* 5, no. 2: 48. https://doi.org/10.3390/urbansci5020048

Trigg, M, Birch, C, Neal, J, Bates, P, Smith, A, Sampson, C, Yamazaki, D, Hirabayashi, Y, Pappenberger, F, Dutra, E, Ward, PJ, Winsemius, HC, Salamon, P, Dottori, F, Rudari, R, Kappes, M, Simpson, A, Hadzilacos, G & Fewtrell, T (2016) The credibility challenge for global fluvial flood risk analysis, *Environmental Research Letters*, http://dx.doi.org/10.1088/1748-9326/11/9/094014

Van Der Knijff, J. M., Younis, J., & De Roo, A. P. J. (2008). LISFLOOD: a GIS-based distributed model for river basin scale water balance and flood simulation. *International Journal of Geographical Information Science*, *24*(2), 189–212. https://doi.org/10.1080/13658810802549154

Wing, O. E. J., Bates, P. D., Quinn, N. D., Savage, J. T. S., Uhe, P. F., Cooper, A., et al. (2024). A 30 m global flood inundation model for any climate scenario. *Water Resources Research*, 60, e2023WR036460. https://doi.org/10.1029/2023WR036460

Yamazaki, D., Ikeshima, D., Sosa, J., Bates, P. D., Allen, G. H., & Pavelsky, T. M. (2019). MERIT Hydro: A high-resolution global hydrography map based on latest topography dataset. *Water Resources Research*, **55**(6), 5053–5073. **https://doi.org/10.1029/2019WR024873**

Zsoter, E., Harrigan, S., Barnard, C., Wetterhall, F., Ferrario, I., Mazzetti, C., Alfieri, L., Salamon, P., Prudhomme, C. (2021): River discharge and related historical data from the Global Flood Awareness System, v3.1. European Commission, Joint Research Centre (JRC). DOI: 10.24381/cds.a4fdd6b9